OBSERVATION OF THE INTERNAL STATES OF A PEMFC ANODE GAS CHANNEL

J. Luna[1]
jluna@iri.upc.edu

C. Batlle[2], C. Kunusch[1], J. Riera[1], M.L. Sarmiento-Carnevali[1], M. Serra[1]
[1]Institut de Robòtica I Informàtica Industrial (UPC-CSIC), C/ Llorens i Artigas 4-6, 08028 Barcelona
[2]Departament de Matemàtica Aplicada IV, Universitat Politècnica de Catalunya, EPSEVG,
Av. V. Balaguer s/n, 08800 Vilanova I la Geltrú

Abstract

In this work a non-linear state observer is developed to estimate the concentrations of the different species inside a Proton Exchange Membrane Fuel Cell (PEMFC) anode gas channel. The implementation of the observer is based on the partial differential equations that define the dynamics of the system, taking into account spatial variations along the anode channel. Forward and backward discretization of the distributed model are employed to take advantage of the boundary conditions of the problem. For comparative reasons, linear and non-linear observability conditions are analysed, and a linear and a non-linear observer are designed. Likewise, two types of Sliding Mode corrective control actions (quasi continuous and super twisting input actions) are implemented in the non-linear state observer. Simulation results are presented to show the performance of the observers and the superiority of the non-linear one over the linear one can be clearly seen.

Keywords: PEMFC, distributed model, non-linear observers, super-twisting, sliding mode

1 INTRODUCTION

Fuel cells are an interesting alternative for clean energy production. Particularly, Proton Exchange Membrane Fuel Cells (PEMFC), with a high power density, are very promising for mass market applications such as automotive and stationary combined heat and power systems. Currently, researchers from all over the world are dedicating a great effort to improve efficiency, reduce degradation and decrease production costs of this technology. In the automatic control field, new estimation, diagnosis and control systems are being developed. In order to design appropriate controllers, different physical variables have to be known. While some of these variables are measurable with the current existing sensor technology, there are parts of the system that are inaccessible. This is the case of the gas channels, where only the inlet and outlet gas flows can be known. Changes in the gases concentrations and temperatures have significant effects on the PEMFC performance and may affect its durability. These variables exhibit a spatial variation in the direction of the channels of the anode and cathode which must be taken into account. The objective of this work is to obtain state observers that provide critical information about the dynamic behavior of the unknown internal states through the reconstruction from the available output measurements of the system. In spite of the industrial interest, research on state estimation in PEMFC is still incipient. Only few works have been published in this topic, mainly addressing the estimation of the oxidant flow and the humidity and water content in membranes and electrodes [2], [7]. In this work, a linear and a non-linear state observer are developed to estimate the concentrations of hydrogen and water vapour in the midpoint of the anode of a PEMFC. The observers are based on a 1D-model with spatial derivatives along the channel [6]. The linear observer is based on a Luenberger state estimation observer structure while the non-linear observer is based on the works of Davila et. al. [1], Levant [3] and Moreno et. al. [5].

In **Section 2** the general system description and statement of the problem is presented. In **Section 3** the mathematical model of the plant based on distributed parameters. In **Section 4** the linear observability is numerically computed for the linearized system and a Luenberger observer is implemented to estimate the states. In **Section 5** the non-linear observability condition is presented and tested for the system and a non-linear observer is developed to reconstruct the hydrogen and water concentrations in the PEMFC anode midpoint. In **Section 6** the results extracted from the simulations are presented and analyzed. Finally, in **Section 7** the conclusions of this work are presented and some future work plans intro-

duced.

2 SYSTEM DESCRIPTION AND PROBLEM STATEMENT

PEM fuel cells produce electrical energy from the consumption of hydrogen and air through an oxidation-reduction chemical reaction. At the anode side the hydrogen is catalytically split into protons and electrons. The protons travel through the electrolyte membrane to react with the air and the returning electrons in the cathode side of the cell, producing water. The electrons travel to the load of the system, producing electrical current through the connection between anode and cathode sides.

The overall system schematic for a single cell PEMFC is represented in Figure 1.

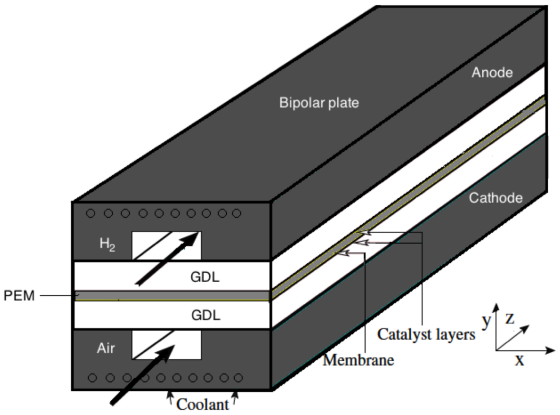

Figure 1: Single PEM cell representation

The work is focused on the anode supply gas channel and the estimation study will be performed in the y-z plane. The spatial derivatives are defined along the z-axis, while the hydrogen and water transport reaction terms are transversal to the supply channel in the y-axis direction. This is showed in the block diagram presented in Figure 2.

It is almost impossible to measure variables inside the gas channels due to the enclosed construction of the PEM fuel cell. Because of this, if we want to design controllers based on the internal states to avoid/reduce degradation in the system, we will need to estimate those values from the available inputs and measurements, which are assumed to be the inlet flow-rates and the outlet concentrations.

The anode gas channel model employed to test the solutions presented in this work has a z-axis length (L) of 0.4 meters and a y-axis channel thickness (δ) of 0.7 mm.

3 MODEL DEVELOPMENT

In this section a mathematical model of the PEMFC anode gas channel will be derived from the partial differential equations of the mass balances, the flow velocities and the pressure drops along the channel's z direction.

$$\frac{\partial c_i}{\partial t} = -\frac{\partial v c_i}{\partial z} - \frac{\dot{n}_i}{\delta} \quad (1)$$

$$v = -K\frac{\partial p}{\partial z} \quad (2)$$

$$p = RT\left(c_{H_2} + c_{H_2O}\right) \quad (3)$$

Table 1 displays all of the variables and parameters used in our study.

Table 1: Nomenclature and units employed

Coefficient	Description, Units
c	Gas concentration, $\frac{mol}{m^3}$
δ	Thickness of the channel, m
K	Pressure drop coefficient, $\frac{m^2}{sPa}$
$\dot{n}$	Molar flux density, $\frac{mol}{m^2 s}$
p	Pressure, Pa
R	Gas constant, $\frac{J}{molK}$
T	Temperature, K
v	Flow velocity, $\frac{m}{s}$
Δz	Discretization length, m

The state variables are the hydrogen (H_2) and water (H_2O) concentrations along the different discretized volumes of the channel. For each gas species, a subscript i will be added to the variables, being $i = 1$ the H_2 index and $i = 2$ the reference for H_2O. A second subscript j will refer to the discretized volume (e.g. $x_{2,2}$ indicates the H_2O concentration in the second volume of discretization).

To make use of the known boundary conditions of the system (input molar fluxes and external ambient pressure), a two-direction discretization will be applied to the spatial partial differential equations that define the dynamics of the system. This discretization,used on equations (1), (2) and (3) yields the following set of equations

$$\dot{x}_{i,j} = \frac{v_{j-1}x_{i,j-1}}{\Delta z} - \frac{v_j x_{i,j}}{\Delta z} - \frac{\dot{n}_{i,j}}{\delta} \quad (4)$$

$$v_j = \frac{K}{\Delta z}\left(p_j - p_{j+1}\right) \quad (5)$$

$$p_j = RT\left(x_{1,j} + x_{2,j}\right) \quad (6)$$

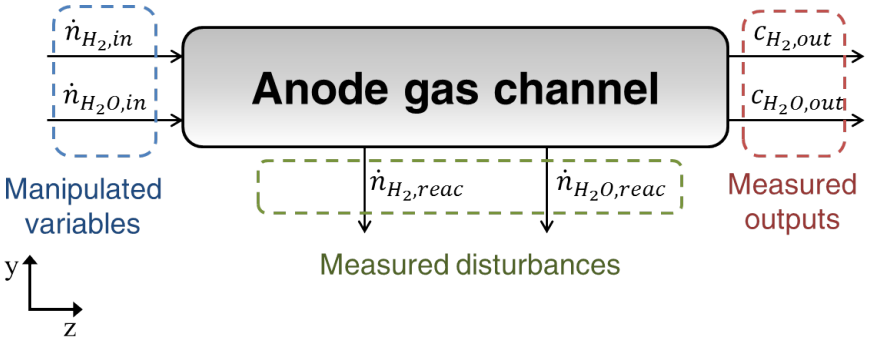

Figure 2: PEMFC anode gas channel model and variables involved in the observation problem

In this work we consider only two discretized volumes along the z axis, and (5) and (6) into (4) result in a 4-dimensional system of the form

$$\begin{aligned}
\dot{x}_{1,1} &= \frac{\dot{n}_{1,in}}{\Delta z} - f_1(\mathbf{x}) - \frac{\dot{n}_{1,1}}{\delta} \\
\dot{x}_{2,1} &= \frac{\dot{n}_{2,in}}{\Delta z} - f_2(\mathbf{x}) - \frac{\dot{n}_{2,1}}{\delta} \\
\dot{x}_{2,1} &= f_1(\mathbf{x}) - f_3(\mathbf{x}) - \frac{\dot{n}_{1,2}}{\delta} \\
\dot{x}_{2,2} &= f_2(\mathbf{x}) - f_4(\mathbf{x}) - \frac{\dot{n}_{2,2}}{\delta}
\end{aligned} \tag{7}$$

where the f_i are state-dependent functions that define the non-linear dynamics of the system, and are given by

$$\begin{aligned}
f_1(\mathbf{x}) &= C_1\left(x_{1,1}^2 + x_{2,1}x_{1,1} - x_{1,2}x_{1,1} - x_{2,2}x_{1,1}\right) \\
f_2(\mathbf{x}) &= C_1\left(x_{1,1}x_{2,1} + x_{2,1}^2 - x_{1,2}x_{2,1} - x_{2,2}x_{2,1}\right) \\
f_3(\mathbf{x}) &= C_1\left(x_{1,2}^2 + x_{2,2}x_{1,2}\right) + C_2 x_{1,2} \\
f_4(\mathbf{x}) &= C_1\left(x_{1,2}x_{2,2} + x_{2,2}^2\right) + C_2 x_{2,2}
\end{aligned} \tag{8}$$

The constants C_1 and C_2 are defined as a combination of the model's parameters that were presented in Table 1

$$C_1 = \frac{K}{\Delta z^2} RT \tag{9}$$

$$C_2 = \frac{K}{\Delta z^2} p^{amb} \tag{10}$$

Some further assumptions have been considered in our study. On one hand, the manipulated variables are the input molar flux densities both for H_2 and H_2O ($\dot{n}_{i,in}$). The transversal molar flux densities for the hydrogen and the water transport through the channel ($\dot{n}_{i,j}$) are included in the model as measured disturbances. Also, the temperature will be considered constant along the channel.

Our study can be generalized to the case of n discretized volumes along the gas channel. In Figure 3 the main structure of the system for this generalization is presented.

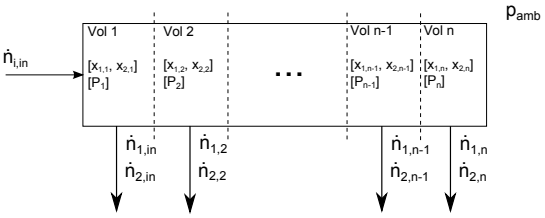

Figure 3: Generalized model of the anode gas channel

4 LINEAR OBSERVABILITY

Before analyzing the non-linear observability of the developed model, a linearization around an operating point $\mathbf{x_0}$ will be performed. From the linearization, the state space representation matrices A, B, C and D will be extracted in order to test the observability of the system around the working point showed in Table 2.

Table 2: Parameters for the linearization

Variable	Value
$\dot{n}_{1,in}$	$35\ \frac{mol}{m^2 s}$
$\dot{n}_{2,in}$	$10\ \frac{mol}{m^2 s}$
$\dot{n}_{1,1}$	$8.1 \cdot 10^{-3}\ \frac{mol}{m^2 s}$
$\dot{n}_{2,1}$	$-1.1243 \cdot 10^{-5}\ \frac{mol}{m^2 s}$
$\dot{n}_{1,2}$	$1.36 \cdot 10^{-2}\ \frac{mol}{m^2 s}$
$\dot{n}_{2,2}$	$-2.5247 \cdot 10^{-6}\ \frac{mol}{m^2 s}$

For linear systems in state space representation, the observability can be tested computing the rank of the observability matrix

$$\mathcal{O} = \begin{bmatrix} C \\ CA \\ \vdots \\ CA^{n-1} \end{bmatrix} \tag{11}$$

If the rank of (11) is equal to the number of states, it is said that the linear system is **observable** around the working point $\mathbf{x_0}$. Making these computations for the linearization of (7) around the point presented in Table 2 one gets that $rank(\mathcal{O}) = 4$ and hence, since our 2-volume system is 4-dimensional, it is possible to reconstruct the states from the information given by the outputs of the system. A simple Luenberger state observer has been implemented to obtain this reconstruction of $\mathbf{x_0}$ from the outputs of the system.

To test the behavior of the observer, simulation have been performed with input inlet gasses variations at times equal to 1 and 2.5 seconds. Besides that, a sinusoidal perturbation is added at time equal to 4 seconds to one of the measured disturbances signals. Results for the estimation of the linear model non-measured states are presented in Figure 4 and Figure 5.

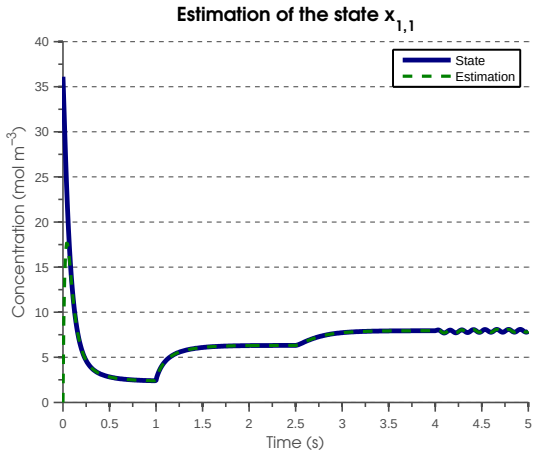

Figure 4: Linear state reconstruction of $x_{1,1}$

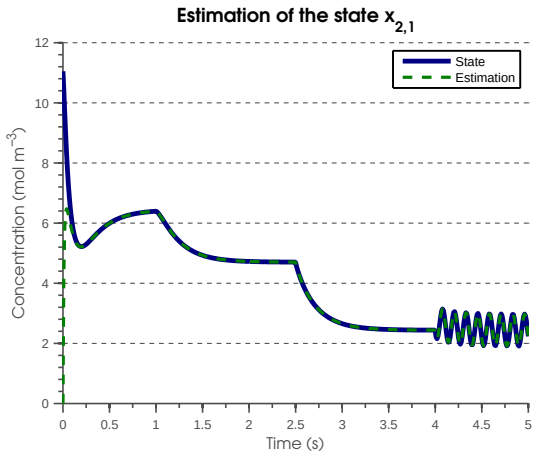

Figure 5: Linear state reconstruction of $x_{2,1}$

As expected from this classic proportional state estimator, the convergence to the unmeasured concentrations occurs very quickly and with no observation error, no matter the inlet gasses variations or the input disturbances applied to the linearized system.

5 NON-LINEAR OBSERVABILITY

Consider a non-linear dynamical system

$$\begin{aligned} \dot{\mathbf{x}} &= \mathbf{f}(\mathbf{x}, \mathbf{u}) \\ \mathbf{y} &= \mathbf{h}(\mathbf{x}) \end{aligned} \tag{12}$$

with state vector $\mathbf{x} \in \Re^n$, input vector $\mathbf{u} \in \Re^m$ and the scalar output vector $\mathbf{y} \in \Re^p$. The non-linear observer structure takes the known nominal part of (12) and a correction term to converge to the states in finite-time.

The main structure of the observer is defined as follows

$$\begin{aligned} \dot{\hat{\mathbf{x}}} &= \mathbf{f}(\hat{\mathbf{x}}, \mathbf{u}) + \mathbf{g}(\hat{\mathbf{x}})\mathbf{u_o} \\ \hat{\mathbf{y}} &= \mathbf{h}(\hat{\mathbf{x}}) \end{aligned} \tag{13}$$

with observed state vector $\hat{\mathbf{x}} \in \Re^n$ and observed output variable $\hat{\mathbf{y}} \in \Re^p$. The vector function $\mathbf{g}(\cdot)$ and the correction observer input $\mathbf{u_o}$ will be designed following the methodology presented in [1].

5.1 OBSERVABILITY ANALYSIS

In the non-linear case, the observation matrix $\mathcal{O}$ is defined by the space containing all repeated Lie derivatives of the output vector field $\mathbf{y}$

$$\mathcal{O}(\mathbf{x}) = \frac{\partial}{\partial \mathbf{x}} \begin{bmatrix} h(\mathbf{x}) \\ L_{f(\mathbf{x})}h(\mathbf{x}) \\ \vdots \\ L^{n-2}_{f(\mathbf{x})}h(\mathbf{x}) \\ L^{n-1}_{f(\mathbf{x})}h(\mathbf{x}) \end{bmatrix} \tag{14}$$

where the Lie derivate evaluates the mapping between the output vector field and the states of the non-linear system presented in (12), and is given by

$$L_{f(\mathbf{x})}h(\mathbf{x}) = \frac{\partial h(\mathbf{x})}{\partial \mathbf{x}} f(\mathbf{x}) \tag{15}$$

To guarantee the observability of (12), the matrix (14) has to be non-singular (full rank). This means that each state variable of the non-linear

system has to have a mapping from the output derivatives to its initial state $x(t_0)$ that distinguishes it from any other initial state x_0.

For the system described in (7), the computation of (14) can be done according to several combinations since there are two measured states. From all these possible combinations, we select the following one, which yields an observation matrix with relative degree equal to 1

$$\mathcal{O}(\mathbf{x}) = \frac{\partial}{\partial \mathbf{x}} \begin{bmatrix} y_1 \\ \dot{y}_1 \\ y_2 \\ \dot{y}_2 \end{bmatrix} = \frac{\partial}{\partial \mathbf{x}} \begin{bmatrix} h_1(\mathbf{x}) \\ L_{f(\mathbf{x})}h_1(\mathbf{x}) \\ h_2(\mathbf{x}) \\ L_{f(\mathbf{x})}h_2(\mathbf{x}) \end{bmatrix} \quad (16)$$

The observability matrix (16) allows to implement corrective control actions for (13) that can also be used to implement closed-loop control on dynamical systems with relative degree equal to 1. Several possibilities are discussed in the literature, and some of them will be compared in this work.

Developing (16) for (7) the following observabiility matrix is obtained

$$\mathcal{O}(\mathbf{x}) = \begin{bmatrix} 0 & 0 & 1 & 0 \\ b_1 & b_2 & b_3 & b_4 \\ 0 & 0 & 0 & 1 \\ d_1 & d_2 & d_3 & d_4 \end{bmatrix} \quad (17)$$

with

$$\begin{aligned} b_1 &= C_1(2x_{1,1} + x_{2,1} - x_{1,2} - x_{2,2}) \\ b_2 &= C_1 x_{1,1} \\ b_3 &= -C_1 x_{1,1} - C_1(2x_{1,2} + x_{2,2}) + C_2 \\ b_4 &= -C_1 x_{1,1} - C1 x_{1,2} \\ d_1 &= C_1 x_{2,1} \\ d_2 &= C_1(x_{1,1} + 2x_{2,1} - x_{1,2} - x_{2,2}) \\ d_3 &= -C_1 x_{2,1} - C_1 x_{2,2} \\ d_4 &= -C_1 x_{2,1} - C_1(x_{1,2} + 2x_{2,2}) + C_2 \end{aligned} \quad (18)$$

As it was introduced before, the rank of (17) has to be equal to n, in this case 4, since this is the number of states of the studied system. The rank of such matrix only depends on the rank of

$$\mathcal{O}_p(\mathbf{x}) = \begin{bmatrix} b_1 & b_2 \\ d_1 & d_2 \end{bmatrix} \quad (19)$$

The rank of (19) must be 2 in order to have full rank in $\mathcal{O}(\mathbf{x})$. This condition will be met only and only if $det\left(\mathcal{O}_p(\mathbf{x})\right) \neq 0$. It may happen that at a given time the previous condition does not hold, and hence, by continuity, the determinant might be very close to zero for some time, in practice making the system non observable during a finite period of time. The solution is to disconnect the observer while the determinant is zero or very small, and to reconnect it afterwards.

5.2 NON-LINEAR OBSERVER

With the observability matrix computed for the non-linear case, it is possible to obtain the $g(\hat{\mathbf{x}})$ vector field of the observer. This procedure is based on the decoupling of the state reconstruction problem, stated by the expression

$$g(\hat{\mathbf{x}}) = \mathcal{O}^{-1}(\hat{\mathbf{x}})[0, 0, \ldots, 1]^T \quad (20)$$

which in our case is

$$g(\hat{\mathbf{x}}) = \begin{bmatrix} \frac{\hat{x}_{1,1}}{det(\mathcal{O}_p(\hat{\mathbf{x}}))} \\ \frac{2\hat{x}_{1,1} + \hat{x}_{2,1} - \hat{x}_{1,2} - \hat{x}_{2,2}}{det(\mathcal{O}_p(\hat{\mathbf{x}}))} \\ 0 \\ 0 \end{bmatrix} = \begin{bmatrix} g_1(\hat{\mathbf{x}}) \\ g_2(\hat{\mathbf{x}}) \\ 0 \\ 0 \end{bmatrix} \quad (21)$$

This result shows again the importance of having a full rank in the observability matrix. The determinant of $\mathcal{O}_p$ is located in the denominator of the uncoupled vector field $g(\hat{\mathbf{x}})$. If this denominator goes to zero, the observability tracking is lost during an unknown period of time. It can also be noticed that, as expected, there is no need to introduce corrective actions for the observation of the states $x_{1,2}$ and $x_{2,2}$ since they are the measured outputs of the system.

Substituting (21) and the estimation of (8) in the generalized state observer (13), the non-linear observer for each of the states can be defined as

$$\begin{aligned} \hat{x}_{1,1} &= \frac{\dot{n}_{1,in}}{\Delta z} - f_1(\hat{\mathbf{x}}) - \frac{\dot{n}_{1,1}}{\delta} + g_1(\hat{\mathbf{x}})u_{1,1} \\ \hat{x}_{2,1} &= \frac{\dot{n}_{2,in}}{\Delta z} - f_2(\hat{\mathbf{x}}) - \frac{\dot{n}_{2,1}}{\delta} + g_2(\hat{\mathbf{x}})u_{2,1} \\ \hat{x}_{1,2} &= f_1(\hat{\mathbf{x}}) - f_3(\hat{\mathbf{x}}) - \frac{\dot{n}_{1,2}}{\delta} \\ \hat{x}_{2,2} &= f_2(\hat{\mathbf{x}}) - f_4(\hat{\mathbf{x}}) - \frac{\dot{n}_{2,2}}{\delta} \end{aligned} \quad (22)$$

It only remains to design the corrective input actions of $\hat{x}_{1,1}$ and $\hat{x}_{2,1}$. As it was introduced before, the relative degree of the system is equal to 1 for each of the output vector fields ($h_1(\mathbf{x})$ and $h_2(\mathbf{x})$) in the observation matrix $\mathcal{O}(\mathbf{x})$. From this we can implement some suitable control actions

that are being used nowadays in closed-loop control of non-linear systems. In particular, for this work, two approaches will be considered

- Quasi-continuous sliding controller [3]
- Super-Twisting algorithm [5]

Both control actions show sliding dynamics based on sign switching functions. For both of them the output observation error e_y will be selected as the sliding surface.

The dynamics of the second order quasi-continuous controller developed in [3] are

$$u_{1,j} = -\alpha \frac{\dot{e}_y + |e_y|^{\frac{1}{2}} sign(e_y)}{|\dot{e}_y| + |e_y|^{\frac{1}{2}}} \tag{23}$$

Following the work presented in [5], we may introduce also the so called Super-Twisting algorithm, defined by

$$\begin{aligned} u_{1,j} &= -K_1 |e_y|^{\frac{1}{2}} sign(e_y) + v \\ \dot{v} &= -K_2 \frac{1}{2} sign(e_y) \end{aligned} \tag{24}$$

In the next section the non-linear observer (22) will be tested for both corrective input actions (23) and (24) in order to compare the obtained results and extract some conclusions.

6 SIMULATION RESULTS AND DISCUSSION

The designed non-linear observer will be put under the same simulation conditions as the linear case showed in section 4. This means that the input inlet gasses values of the system will be varied at time equal to 1 and 2.5 seconds. On the other hand, a sinusoidal perturbation will be added at time equal to 4 seconds.

The results of the performed simulations are presented in Figure 6 and Figure 7. The simulation has been computed for the two variants of the non-linear state observer. Besides, the linear observer has been put into use to test if it can reconstruct the non-linear states.

In the simulation results the linear states of the system, for the same inputs and disturbances variations, are also showed in order to compare the results with the dynamic behaviour of the non-linear system.

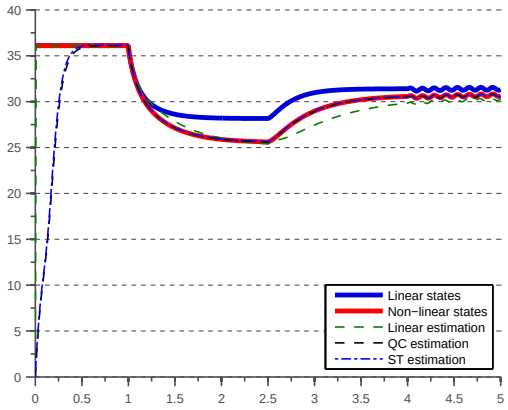

Figure 6: Non-linear state reconstruction of $x_{1,1}$

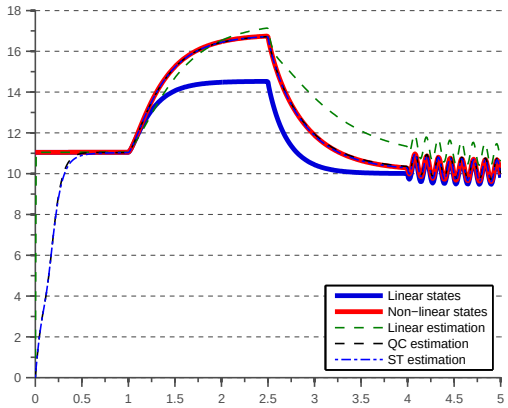

Figure 7: Non-linear state reconstruction of $x_{2,1}$

It can be inferred from Figure 6 and Figure 7 that the linear observer is unable to follow the trajectory of the non-linear dynamics. This justifies the need to develop the non-linear state observer presented in this work. Besides that, both corrective actions for the non-linear observer show similar dynamical responses, and they both converge to the states in finite-time.

The difference between the value of the state and the estimated value is the reconstruction error. For the unmeasured states $x_{1,1}$ and $x_{2,1}$, the state reconstruction error is showed in Figure 8 and Figure 9, where it is showed that the reconstruction error goes to zero in a relatively short time (around 1.5 seconds after the beginning of the simulation).

On the other hand, the simulation results show that for the same values of the inputs and the known disturbances, the behaviour of the linearized system is different from the non-linear model of the plant. In particular, an offset exists between both dynamical responses.

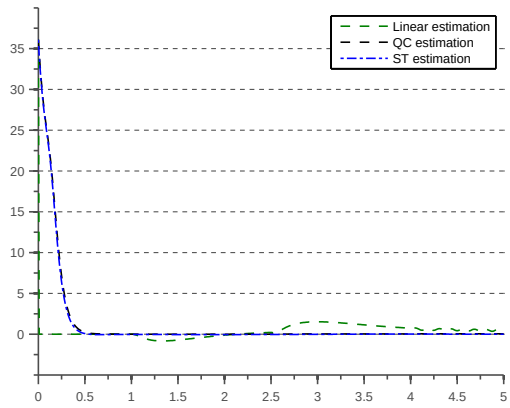

Figure 8: State reconstruction error of $x_{1,1}$

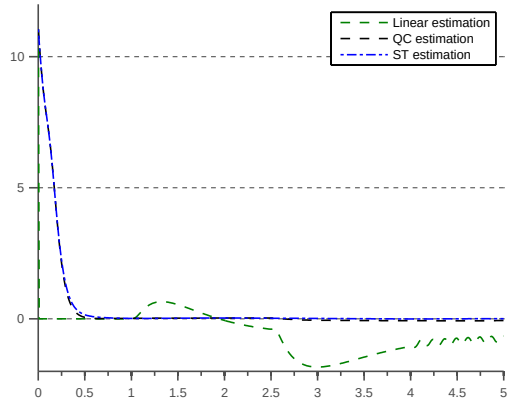

Figure 9: State reconstruction error of $x_{2,1}$

7 CONCLUSIONS

While the linearization of the system may allow us to work at a certain operating point with a linear model, the constantly changing conditions of PEMFC-based systems make necessary to use the full non-linear description. Our work shows that there exists an offset between both models (linear and non-linear), and the complete state representation has to be employed to fully understand the behaviour of the plant.

The physical construction of the fuel cell makes it impossible to know the evolution of the inside concentrations values with time, and a state observer has to be implemented to estimate these concentrations. The linear observer never converges to the non-linear response, making it necessary to implement the non-linear observer model that was developed for this particular application.

The observability matrix has been constructed from the mapping of the outputs with a relative degree equal to 1. This allows the implementation of the studied corrective sliding control actions that have been presented in this work. For higher numbers of discretized volumes, or for other combinations of the observability matrix, new controllers will have to be implemented.

Up until this point, all the disturbances of the system have been considered known beforehand. In reality, the estimation of the water transport inside the channel (and the rest of the PEMFC) is a complex task. In future work, it is planned to analyze the degree of model and input uncertainties that can be included into the design of the non-linear observer.

It is also interesting to remark that, while in the present work only 2 discretized volumes have been considered, the goal is to generalize the approach up to n volumes. This way, a complete and detailed profile of the hydrogen and water concentrations can be extracted with only the output values in the last discretized volume. This is theoretically possible because of the sequential structure of the model but numerical complications arise when the number of discretized volumes increases. This detailed information will be useful to implement controllers in the system in order to maximize efficiency and avoid degradation.

Finally, it has to be clarified that this work presents the approach for the observation in the anode layer of the fuel cell. In the future, the rest of the PEMFC components (anode, membrane, etc.) will be added to the model and more state observers will be designed to extract additional information of the system dynamics.

Acknowledgements

This work has been supported by national project MESPEM with reference DPI2011-25649.

References

[1] Davila J., Fridman L., Pisano A., Usai E., (2008), "Finite-time state observation for non-linear uncertain systems via higher-order sliding modes", *Internation Journal of Control*, vol 82, no 8.

[2] Kazmi I.H., Bhatti A.I. Iqbal S.A., (2009), "A non-linear observer for PEM fuel cell system", *IEEE 13th International Multitopic Conference (INMIC)*

[3] Levant A. (2005), "Quasi-Continuous High-Order Sliding-Mode Controllers", *IEEE Transactions on Automatic Control*, vol 50, no 11.

[4] Mangold M., Bück A., Hanke-Rauschenbach R., (2010), "Passivity based control of a distributed PEM fuel cell model", *Journal of Process Control*, vol 20, pp 292-313.

[5] Moreno, J. A., Osorio, M. A., (2008). "A lyapunov approach to second-order sliding mode controller and observers", *Proceedings of the 47th IEEE Conference on Decision and Control*

[6] Sarmiento-Carnevali M., Serra M., Batlle C., (2013) "Distributed parameter model simulation tool for PEM fuel cells", *International Journal of Hydrogen Energy.* DOI:10.1016/j.ijhydene.2013.04.015

[7] Thawornkuno C., Panjapornpon C., (2008) "Estimation of Water Content in PEM Fuel Cell", *Chiang Mai J. Sci*, 35(1): 212-220